Near-IR Irradiation of the S_2 State of the Water Oxidizing Complex of Photosystem II at Liquid Helium Temperatures Produces the Metalloradical Intermediate Attributed to $S_1Y_Z^{\bullet}$ †

Dionysios Koulougliotis,[‡,||] Jian-Ren Shen,[§] Nikolaos Ioannidis,[‡] and Vasili Petrouleas*[,‡]

Institute of Materials Science, NCSR "Demokritos", 153 10 Aghia Paraskevi Attikis, Greece, Department of Biochemistry and Biotechnology, University of Thessaly, Ploutonos 26 and Aiolou, 41221, Larissa, Greece, RIKEN Harima Institute and PRESTO, JST, Mikazuki-cho, Sayou-gun, Hyogo 679-5148, Japan

Received October 22, 2002; Revised Manuscript Received January 21, 2003

ABSTRACT: Near-IR (NIR) excitation at liquid He temperatures of photosystem II (PSII) membranes from the cyanobacterium *Synechococcus vulcanus* or from spinach poised in the S_2 state results in the production of a $g = 2.035$ EPR resonance, reminiscent of metalloradical signals. The signal is smaller in the spinach preparations, but it is significantly enhanced by the addition of exogenous quinones. Ethanol (2−3%, v/v) eliminates the ability to trap the signal. The $g = 2.035$ signal is identical to the one recently obtained by Nugent et al. by visible-light illumination of the S_1 state, and preferably assigned to $S_1Y_Z^{\bullet}$ [Nugent, J. H. A., Muhiuddin, I. P., and Evans, M. C. W. (2002) *Biochemistry 41*, 4117−4126]. The production of the $g = 2.035$ signal by liquid He temperature NIR excitation of the S_2 state is paralleled by a significant reduction (typically 40−45% in *S. vulcanus*) of the S_2 state multiline signal. This is in part due to the conversion of the Mn cluster to higher spin states, an effect documented by Boussac et al. [Boussac, A., Un, S., Horner, O., and Rutherford, A. W. (1998) *Biochemistry 37*, 4001−4007], and in part due to the conversion to the $g = 2.035$ configuration. Following the decay of the $g = 2.035$ signal at liquid helium temperatures (decay halftimes in the time range of a few to tens of minutes depending on the preparation), annealing at elevated temperatures (−80 °C) results in only partial restoration of the S_2 state multiline signal. The full size of the signal can be restored by visible-light illumination at −80 °C, implying that during the near-IR excitation and subsequent storage at liquid helium temperatures recombination with Q_A^- (and therefore decay of the S_2 state to the S_1 state) occurred in a fraction of centers. In support of this conclusion, the $g = 2.035$ signal remains stable for several hours (at 11 K) in centers poised in the $S_2 \cdots Q_A$ configuration before the NIR excitation. The extended stability of the signal under these conditions has allowed the measurement of the microwave power saturation and the temperature dependence in the temperature range of 3.8−11 K. The signal intensity follows Curie law temperature dependence, which suggests that it arises from a ground spin state, or a very low-lying excited spin state. The $P_{1/2}$ (microwave power at half-saturation) value is 1.7 mW at 3.8 K and increases to 96 mW at 11 K. The large width of the $g = 2.035$ signal and its relatively fast relaxation support the assignment to a radical species in the proximity of the Mn cluster. The whole phenomenology of the $g = 2.035$ signal production is analogous to the effects of NIR excitation on the S_3 state [Ioannidis, N., Nugent, J. H. A., and Petrouleas, V. (2002) *Biochemistry 41*, 9589−9600] producing an $S_2'Y_Z^{\bullet}$ intermediate. In the present case, the intermediate is assigned to $S_1Y_Z^{\bullet}$. The NIR-induced increase in the oxidative capability of the Mn cluster is discussed in relation to the photochemical properties of a Mn(III) ion that exists in both S_2 and S_3 states. The EPR properties of the $S_1Y_Z^{\bullet}$ intermediate cannot be reconciled easily with our current understanding of the magnetic properties of the S_1 state. It is suggested that oxidation of tyr Z alters the magnetic properties of the Mn cluster via exchange of a proton.

The light-driven oxidation of water to molecular oxygen in green plants, algae, and cyanobacteria is catalyzed by a membrane−protein complex known as photosystem II (PSII).[1] The core of PSII, where the main photochemistry occurs, consists of two polypeptide chains, D1 and D2, to which a number of electron transport cofactors are attached. Upon photon excitation of a specialized chlorophyll moiety, known as P_{680}, electron flow is initiated during which a Mn cluster acts as an electron donor to P_{680}^+ via the redox active tyrosine 161 of the D1 polypeptide (denoted as tyr Z or Y_Z). Electrons are transferred to the acceptor side, consisting of a pheophytin intermediate and a terminal iron−quinone complex. The Mn cluster (believed to be tetranuclear) and the tyrosine Z, located in the lumenal side of the thylakoid membrane, comprise what is called the oxygen-evolving complex (OEC). The OEC cycles through five

† This work was supported in part by EC Grant ERBFMRX-CT980214 and by the Greek Secretariat of Research and Technology (Grant PENED 99ED75).

* To whom correspondence should be addressed. Telephone: +30 210 650-3344. Fax: +30 210 651-9430. E-mail: vpetr@ims.demokritos.gr.

‡ NCSR "Demokritos".

§ RIKEN Harima Institute and PRESTO.

|| University of Thessaly.

10.1021/bi027051o CCC: $25.00
Published on Web 02/22/2003

intermediate oxidation states, S_0-S_4, during sequential photon absorption by PSII. Oxygen evolves during the S_3 to S_0 transition (S_4 being a transient state). S_0, which is the lowest active oxidation state of the complex, is slowly oxidized in the dark by the distant tyrosine D (known as Y_D) to the dark-stable state, S_1 (see refs *1*−*7* for reviews).

Significant effort has been devoted in recent years to the detection of metalloradical intermediates during the cycling of the OEC. A broadened radical EPR signal, 100−230 G wide (depending on the treatment), was initially observed in PSII preparations in which advancement to the S_3 state was inhibited by calcium depletion, ammonia or acetate treatment, etc. (*8*−*16*). The signal and variants of it were attributed to the $Y_Z^\bullet$ radical interacting with the S_2 state of the Mn cluster ($S_2Y_Z^\bullet$; *13*−*18*), and subsequent theoretical simulations have implied a short distance (≤8 Å) between $Y_Z^\bullet$ and the Mn cluster (*19*−*23*). This is in agreement with the recent X-ray crystallographic data. This proximity is sufficient to imply a direct role of $Y_Z^\bullet$ in the water oxidation process (*1*, *17*, *24*−*26*).

It has been thought that $Y_Z^\bullet$ is too short-lived in intact preparations to be trapped for EPR studies. A growing body of evidence in recent years points, however, to the possibility of trapping this radical at liquid helium temperatures. A broadened radical EPR signal was observed in O_2-evolving PSII preparations following a rather complex protocol, including advancement to higher S states (by cycles of illumination and dark adaptation), prolonged storage at 77 K, and subsequent excitation by white light at 11 K (*27*). A broadened radical signal was also observed following near-IR (NIR) excitation of the S_3 state at cryogenic temperatures (*28*). In a follow-up study, the two signals were assigned to the same intermediate state, $S_2'Y_Z^\bullet$ (*29*), where S_2' is a one-proton-deficient S_2 configuration trapped during the decay of S_3 at cryogenic temperatures (*30*). Visible-light excitation of S_2' in the experiment of Nugent et al. (*27*) caused charge separation, while NIR excitation of S_3 in the experiment of Ioannidis and Petrouleas (*28*) caused backward electron transfer (from tyr Z to the Mn cluster), producing in both cases the same metalloradical intermediate (*29*). A different radical intermediate has been trapped by a pH jump to alkaline pH of samples in the S_3 state. The radical has been assigned to the interaction of $Y_Z^\bullet$ with a doubly deprotonated S_2 configuration of the Mn cluster (*31*).

In a recent straightforward experiment, a new broadened radical EPR signal was detected by illumination with visible light at cryogenic temperatures (<20 K) of O_2-evolving PSII membranes poised in the dark-stable S_1 state (*32*). The signal was assigned to $S_1X^\bullet$, where $X^\bullet$ could be either $Y_Z^\bullet$ (preferred option) or a carotenoid radical ($Car^{\bullet+}$). This new radical signal displays a characteristic $g = 2.035$ narrow absorption-type component accompanied by less well-defined $g \leq 2.0$ components, and decays in the dark either by back reaction with Q_A^- or by forward electron transfer from the Mn cluster, then giving rise to a multiline signal attributed to a "non-relaxed" conformation of the S_2 state. An apparently similar signal was detected in control experiments during the study of the S_3 state involving excitation of S_2 by NIR light (N. Ioannidis and V. Petrouleas, unpublished results).

The sensitivity of the Mn cluster to near-IR light was detected by Boussac et al. (*33*−*35*), who observed that excitation of the S_2 state by NIR light (action spectrum peaking at ~820 nm) at temperatures between 65 and 200 K caused spin transitions in the Mn cluster (*33*, *34*). A similar effect was subsequently observed in the S_3 state (*28*, *29*), but the spin transitions inside the Mn cluster were accompanied in this case by the transfer of the positive hole to tyr Z in a fraction of centers (*28*). These results were reproduced in a cyanobacterial preparation (*36*). The work presented here extends the earlier studies and shows that NIR excitation of the S_2 state at liquid helium temperatures results in production of the same metalloradical intermediate trapped by Nugent et al. (*32*), which is assigned to $S_1Y_Z^\bullet$. The results are discussed on the basis of a model assuming proton exchange between tyr Z and the Mn cluster.

MATERIALS AND METHODS

PSII-enriched membranes from market spinach (BBY preparations) were isolated by standard procedures (*37*, *38*) with some modifications. Samples for EPR measurements were suspended in a pH 6.5 buffer containing 0.4 M sucrose, 15 mM NaCl, and 40 mM MES, at a final chlorophyll concentration of 6−8 mg of Chl/mL, and subsequently stored in liquid nitrogen (N_2). In certain experiments, the BBY membranes were supplemented with exogenous quinones, 1 mM DCBQ or PPBQ, from a stock solution in DMSO. PSII core complexes from *Synechococcus vulcanus* highly active in oxygen evolution were isolated as described previously (*39*, *40*).

Samples were poised in the S_1 state by dark adaptation at 273 K for 1 h. The samples were advanced to the S_2 state by illumination at 200 K for 4−6 min. An 82 V, 360 W OSRAM 93525 halogen projector lamp filtered with a saturated solution of $CuSO_4$ was used. Illuminations at liquid He temperatures were performed directly in the EPR cavity using the same lamp for a maximum of 3 min in intervals of 45 s, to avoid sample heating. A combination of water and a 3 mm RG715 SCHOTT filter (absorbing below 715 nm) was used to select for near-infrared light, while a combination of a 3 mm BG39 filter (absorbing above 650−700 nm) and a saturated $CuSO_4$ solution was employed to select visible light. Poising the Mn cluster at the S_2 multiline state and the primary electron acceptor quinone (Q_A) at the oxidized form, in BBY preparations, was achieved by illumination at 200 K for 6 min, followed by a short period (15 s) of dark incubation at 0 °C and immediate freezing at 77 K in the presence of DCBQ or PPBQ (*41*). Alternatively, the non-heme iron was preoxidized with 5 mM $K_3Fe(CN)_6$ and acted as a stable electron acceptor during charge separation.

EPR measurements were performed with a Bruker ER-200D-SRC spectrometer interfaced with a personal computer

[1] Abbreviations: PSII, photosystem II; OEC, oxygen-evolving complex; WOC, water oxidizing complex; S_0-S_4, oxidation states of the water oxidizing complex; tyr Z or Y_Z and tyr D or Y_D, fast and slow tyrosine electron donors of PSII, respectively; Chl_Z and Car, chlorophyll and carotene, respectively, acting as electron donors in side pathways; Q_A and Q_B, primary and secondary plastoquinone electron acceptors of PSII, respectively; BBY membranes, thylakoid membrane fragments enriched in PSII; MES, 2-(*N*-morpholineethanesulfonic acid); chl, chlorophyll; PPBQ, phenyl-*p*-benzoquinone; DCBQ, 2,5-dichloro-benzoquinone; DMSO, dimethyl sulfoxide; NIR light, near-infrared light; EPR, continuous wave electron paramagnetic resonance; liquid helium temperatures, temperatures well below 77 K reached by the use of liquid helium as a cryogen.

and equipped with an Oxford ESR 900 or ESR 910 cryostat, an Anritsu MF76A microwave frequency counter, and a Bruker 035M NMR gaussmeter. Typically, the spectra that are obtained are averages of two scans, by using 4 mm standard EPR tubes.

The power and temperature dependence of the $g = 2.035$ signal was studied primarily in BBY samples with Q_A poised at the oxidized state. Control experiments with samples from *S. vulcanus* were subjected to small corrections for the decay of the signal during the experiments. The temperature was calibrated with a thermocouple placed inside a test sample. A separate control of the temperature was provided by comparison with the temperature variation of tyr $D^{\bullet}$. The microwave power at half-saturation ($P_{1/2}$) of the $S_1Y_Z^{\bullet}$ signal was calculated from a least-squares fit of the signal amplitude (S) versus the microwave power P with eq 1

$$S = kP_{1/2}/(1 + P/P_{1/2})^{b/2} \quad (1)$$

where k is a scaling constant and the parameter b was fixed at 1 (limit of totally inhomogeneous line broadening).

RESULTS

A Broadened g = 2.035 Radical Signal Is Induced by NIR Excitation of the S_2 State at Liquid Helium Temperatures. Samples prepared in the S_2 state have an unusual sensitivity to NIR excitation, as was originally detected by Boussac et al. (*33*−*35*). The Mn multiline signal arising from an $S = {}^1/_2$ manifold converts in a large part to higher-spin states. The effect is more pronounced in the presence of 2−3% ethanol which enhances the fraction of centers in the $S = {}^1/_2$ configuration. It is shown below that NIR excitation at temperatures close to 4.2 K of samples prepared in the S_2 state induces a broadened radical signal. Experiments were performed in two types of preparations, a cyanobacterial preparation from *S. vulcanus* and a PSII membrane preparation from spinach.

Figure 1 summarizes the experimental observations on the PSII core complex isolated from *S. vulcanus*. If one starts with complexes poised in the S_1 state, illumination at 200 K for 4 min causes advancement to the S_2 state (Figure 1A) which is concomitant with the reduction of the quinone−iron, Q_AFe^{2+}, electron acceptor. In these cyanobacterial preparations, the S_2 state is characterized by the multiline EPR signal centered at $g = 2$ and no $g \approx 4$ signal (*35*). Other features in the difference spectra include the $Q_A^-Fe^{2+}$ signal at $g \approx 1.9$ and negligible contributions at $g = 3$ due to cytochromes c_{550} and b_{559}. Illumination at 5 K with NIR light for 3 min (Figure 1B) induces several changes. The amplitude of the S_2 state multiline signal is reduced by approximately 45%. This is accompanied by the formation of a sharp signal at $g = 2.035$. A broad EPR signal at $g \approx 5-9$ can be also discerned in the 5-fold expanded traces. The latter is attributed to the formation of high-spin states ($S = {}^5/_2$) of the Mn complex in a fraction of centers due to the NIR illumination (*35*). A small portion of this signal appeared to exist already in the S_2 state spectrum of Figure 1A. Sample incubation at ∼35 K for 30 min (Figure 1C) results in complete decay of the $g = 2.035$ signal.

In the experiments of Boussac et al. (*33*−*35*), the original multiline signal intensity was restored following storage for a few seconds at 200 K. Figure 1D shows the spectrum

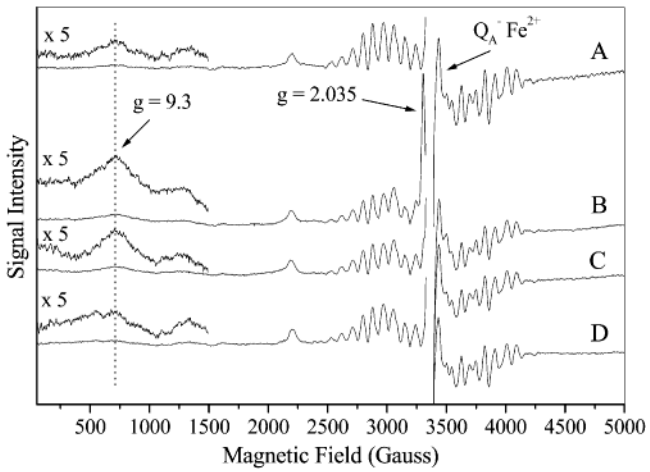

FIGURE 1: Production and decay of the $g = 2.035$ signal in PSII core complexes from *S. vulcanus*. The EPR spectra are the average of four independent data sets. The following sequential treatments are shown: (A) illumination at 200 K for 4 min of a sample poised in the S_1 state, (B) illumination of the S_2 state at 5 K with near-IR light for a period of 3 min, (C) dark incubation for 30 min at 35 K in the EPR cavity, and (D) dark incubation at −80 °C for 5 min. The EPR spectrum of the initial dark-stable S_1 state has been subtracted from all spectra. EPR conditions were as follows: 11 K, microwave frequency of 9.41 GHz, microwave power of 38 mW, and modulation amplitude of 25 G. The insets are the same spectra multiplied by a factor of 5 to distinguish the spectral details. The $g = 2.035$ signal induced by NIR illumination, the Q_A^-−Fe^{2+} signal, and the broad $g = 9.3$ EPR signal are denoted by arrows. The central region at $g = 2.0$ has been omitted for clarity.

recorded following a subsequent incubation of the sample at −80 °C for a period of 5 min. The $g \approx 9$ signal decays to the initial level, but the multiline signal is not fully restored. While part of this decreased intensity could be attributed to the noncomplete conversion of the $g = 5-9$ signal, it can be noted that the $Q_A^-Fe^{2+}$ signal is also smaller compared to Figure 1A. Quantitations of the latter signal cannot be accurate, however, because of the overlap with the multiline signal and with a potential negative contribution of the $g = 2.035$ signal in Figure 1B. Further illumination at 200 K results in restoration of the size of the signals in Figure 1A (data not shown). In a separate control experiment (not shown), storage of the $S_2Q_A^-$ state at −80 °C for a similar period of time did not result in any noticeable charge recombination. These observations suggest that the low-temperature NIR excitation followed by the subsequent storage at 35 K resulted in charge recombination in a fraction of centers. This phenomenology is similar to the effects of NIR excitation of the S_3 state (*30*). Additional evidence for this effect will be provided later.

Similar results were obtained with PSII preparations from spinach. These are summarized in Figure 2.

The spectrum in Figure 2A represents the S_2 state obtained by illumination at 200 K, exhibiting contributions from both the multiline and the $g = 4.1$ signal configurations. NIR illumination of this state at liquid He temperatures results in a decrease in the magnitude of the multiline signal (by ca. 40% in this experiment) as evidenced from the difference spectrum (NIR illuminated minus S_2 state) (Figure 2B) displaying an inverse multiline EPR signal. In addition, a small $g = 2.035$ signal is induced. The latter signal is significantly enhanced (by a factor of 3−3.5) in samples supplemented with 1 mM DCBQ (Figure 2C) or PPBQ (data

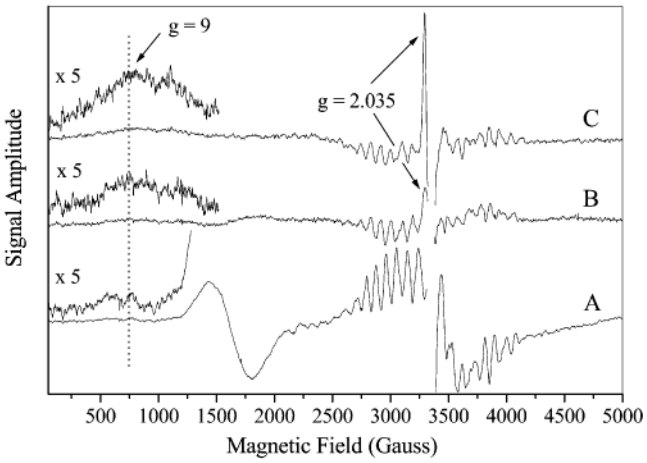

FIGURE 2: Production of the $g = 2.035$ signal in PSII membranes from spinach and enhancement of the signal size by the addition of DCBQ. The following spectra are shown: (A) the S_2 state multiline signal produced by illumination at 200 K for 3 min of a sample poised in the S_1 state (the spectrum of the initial dark-stable S_1 state has been subtracted), (B) changes induced by subsequent excitation by NIR light at 5 K for 3 min (the spectrum of the S_2 state has been subtracted), and (C) the difference spectrum as in part B but after initial addition of 1 mM DCBQ. EPR conditions were as described in the legend of Figure 1. The central region at $g = 2.0$ has been omitted for clarity. The insets are the same spectra multiplied by a factor of 5 to enhance the weak low-field spectral details.

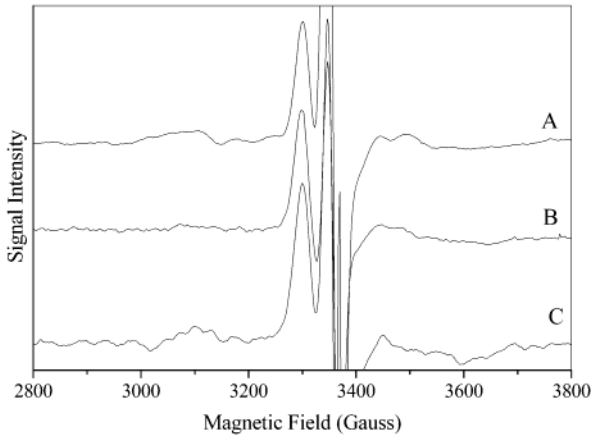

FIGURE 3: Production of the $S_1Y_Z^{\bullet}$ signal in *S. vulcanus* PSII preparations (A) or spinach BBY particles (B and C) by illumination at 5 K in the EPR cavity for a period of 3 min. In each case, the signal was produced by the following procedures: (A and B) NIR light starting with a sample poised at the S_2 state and (C) visible light starting with the same sample as in part B poised at the S_1 state. The EPR spectrum obtained after dark incubation at −80 °C for 3−5 min of each sample following NIR illumination has been subtracted from all EPR spectra. EPR conditions were the same as those described in the legend of Figure 1.

not shown). The contributions from the NIR-induced high-spin signals in the low-field region of the EPR spectra are weak compared to the earlier studies (*33*, *34*), because of the absence of ethanol (ethanol enhances the NIR-sensitive fraction of centers) and the lower temperature of excitation of the samples in the experiments presented here. The spinach samples displayed behavior qualitatively similar to that of the *S. vulcanus* samples during sequential treatments similar to those described for parts C and D of Figure 1.

Experiments similar to those in Figure 2 in the presence of 2−3% ethanol resulted in no $g = 2.035$ signal formation. Also, visible-light excitation of the S_2 state produced ca. 35% of the $g = 2.035$ signal compared to the size of the signal produced by NIR excitation of the same state. Although the action spectrum of the NIR effect was not determined, an approximate window of ∼700−900 nm could be set as in ref *28*.

NIR Excitation of the S_2 State or Visible-Light Excitation of the S_1 State, at Liquid Helium Temperatures, Induces the Same Radical Signal in both Spinach and S. vulcanus Preparations. Figure 3 displays the $g = 2.035$ EPR signal obtained in either *S. vulcanus* (Figure 3A) or spinach (Figure 3B) PSII preparations; samples were initially poised at the S_2 state and subsequently illuminated with NIR light at 5 K. When the same spinach PSII sample is poised at the S_1 state and subsequently illuminated with visible light at 5 K, an identical (in form and position) $g = 2.035$ EPR signal is obtained (Figure 3C). A similar signal, but much smaller in size than the one in Figure 3A, is also induced by visible-light excitation of *S. vulcanus* samples (not shown). The signal induced by visible-light excitation of S_1 was first observed by Nugent et al. (*32*) and assigned to $S_1X^{\bullet}$, where X could be $Y_Z^{\bullet}$ or $Car^{\bullet+}$. Arguments in favor of the first option (assignment to $S_1Y_Z^{\bullet}$) will be presented in the Discussion. It should also be noted that this phenomenology is entirely analogous to the production of the same $S_2'Y_Z^{\bullet}$ intermediate either by NIR excitation of the S_3 state or by visible-light excitation of S_2' (a proton-deficient S_2 configuration) (*29*).

It should be noted that no changes in the signal II level were observed during the production or decay of the $g = 2.035$ signal.

Decay Rate of the Radical Signal. At Liquid Helium Temperatures, the Signal Decays Predominantly via Charge Recombination with Q_A^-. The decay rate of the $g = 2.035$ signal at liquid helium temperatures depends on how it is produced. In agreement with the study of Nugent et al. (*32*) who reported a $t_{1/2}$ of approximately 4 min at 11 K, our experiments indicated a $t_{1/2}$ between 3 and 6 min (data not shown) when the signal is produced by illumination of the S_1 state with visible light. When the $g = 2.035$ signal is produced by NIR illumination of the S_2 state, it decays with a slower rate. Figure 4 (□) shows the decay of the NIR-induced signal in BBY samples supplemented with 1 mM DCBQ. Fitting with biexponential kinetics yields $t_{1/2}$ values of approximately 3 min (45% of the signal) and 50 min (55% of the signal). In PSII membranes isolated from *S. vulcanus*, the decay of the signal is even slower with an average half-time ($t_{1/2}$) of ca. 2 h (data not shown). A notable difference in the samples from *S. vulcanus* was the presence of spontaneously oxidized iron in a fraction of centers.

The decay of the $S_1Y_Z^{\bullet}$ intermediate, produced by visible-light excitation of the S_1 state, has been attributed to charge recombination at liquid helium temperatures, and forward electron transfer, i.e., electron transfer from the Mn cluster to $Y_Z^{\bullet}$ at ≥77 K (*32*). This general motif, charge recombination being favored at liquid helium temperatures and forward electron transfer favored at ≥77 K, was also observed with the intermediate $S_2'Y_Z^{\bullet}$, produced by NIR excitation of the S_3 state or visible-light excitation of the S_2' state (the decay product of S_3 at 77 K) (*29*, *30*). To test the potential influence of the acceptor side on the decay of the NIR-induced $Y_Z^{\bullet}$ signal, the decay rate was also examined in samples where

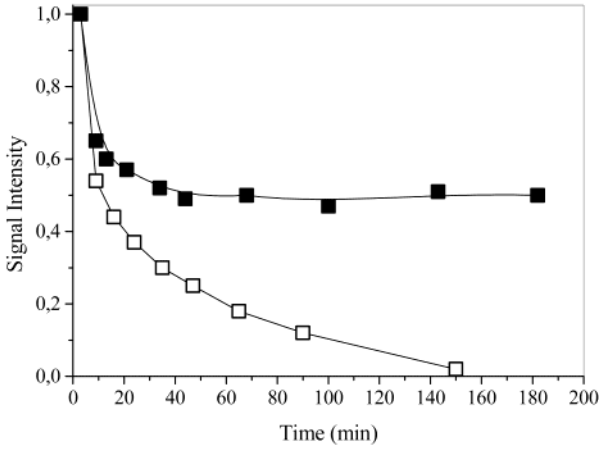

FIGURE 4: Decay kinetics of the $S_1Y_Z^{\bullet}$ signal at 11 K. The signal was induced by NIR illumination of the S_2 state at 5 K. PSII spinach membranes were supplemented with 1 mM DCBQ: (□) samples with reduced, Q_A^-, and (■) samples with oxidized, Q_A. The semiquinone oxidation was achieved by a brief (15 s) incubation at 0 °C of a sample poised at the $S_2\cdots Q_A^-$ state (see Materials and Methods).

Table 1: $P_{1/2}$ Values of the $g = 2.035$ ($S_1Y_Z^{\bullet}$) Signal Calculated from Microwave Power Saturation Data

T (K)	$P_{1/2}$ (mW)
3.8	1.7 ± 0.3
7.0	11 ± 2
11	96 ± 12

Q_A^- was oxidized by short term (15 s) dark adaptation at 0−4 °C of the $S_2\cdots Q_A^-$ state in the presence of the external quinone, DCBQ. The decay of the $g = 2.035$ signal produced by NIR excitation of the $S_2\cdots Q_A$ state is plotted in Figure 4 (■). Clearly, apart from a fast decaying component (resulting presumably from centers in which Q_A^- was not oxidized), a significant nondecaying fraction (55%) exists. Qualitatively similar results were obtained in experiments where the $S_2\cdots Q_A$ state was produced by illumination of the S_1 state in which the non-heme iron was chemically oxidized. The stabilization of the $g = 2.035$ signal in samples with oxidized Q_A strongly indicates that the signal in a significant fraction of centers decays via charge recombination at 11 K. A lower stability of Q_A^- when produced by visible-light excitation of S_1 at liquid helium temperatures could explain the faster decay of the $g = 2.035$ signal compared with its homologue produced by NIR excitation of the S_2 state.

It is more difficult to check the high-temperature (≥77 K) fate of the $S_1Y_Z^{\bullet}$ signal due to the presence of a significant fraction of nonreacted S_2 state signals and the NIR-induced interconversion among them. It is reasonable to assume, however, that at high temperatures forward electron transfer (the normal pathway of decay of the $S_1Y_Z^{\bullet}$ state via conversion to S_2Y_Z) is favored.

Power and Temperature Dependence of the Radical Signal. The slow decay kinetics of the $g = 2.035$ signal produced by NIR illumination of the S_2 state in *S. vulcanus* and its increased stability in BBY membranes with preoxidized Q_A (as described above) allowed for a measurement of its relaxation characteristics via $P_{1/2}$ measurements as well as examination of its temperature dependence. Table 1 gives the $P_{1/2}$ values obtained at three different temperatures. The measurements are in agreement with the preliminary observations of Nugent et al. (*32*) and provide additional evidence for the close association of the radical with a nearby paramagnet, the Mn cluster in the S_1 state. The existence of a paramagnetic form of the S_1 state has been established in the past via indirect (*43*) and direct (*44*−*47*) observations (see the Discussion for further considerations). The $P_{1/2}$ values in Table 1 display magnitudes on the same order with those of the "$S_2Y_Z^{\bullet}$" signal trapped in acetate-inhibited samples (*42*). Direct comparison cannot be made, however, because of the differing spin states of the Mn cluster in the two cases.

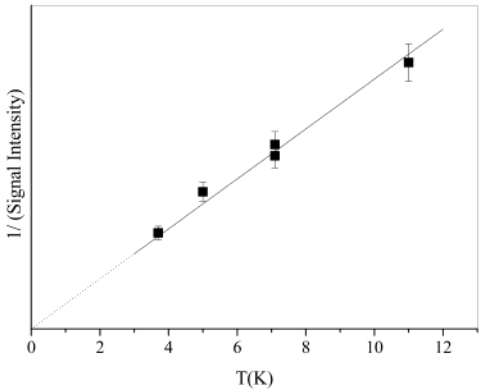

FIGURE 5: Dependence of the inverse intensity of the $S_1Y_Z^{\bullet}$ signal on temperature. The signal intensities are the averages of spectra obtained at two different nonsaturating microwave powers (0.25 and 0.13 mW). The error bars correspond to an uncertainty of 7% in the signal intensity. A linear fit is shown superimposed on the experimental data.

The temperature dependence of the $g = 2.035$ signal intensity at nonsaturating microwave powers is shown in Figure 5. The inverse of the signal intensity varies linearly with temperature (Curie law dependence) in the temperature range that was employed (3.8−11 K). Consequently, it is concluded that the $g = 2.035$ signal results from a ground state, although, due to the limited accuracy of the temperature determination in EPR experiments, one cannot exclude the assignment to a low-lying excited state. It should be noted, however, that no alternative signals attributed to the interaction of the radical with a different spin manifold of the Mn cluster could be detected. Of interest is, in particular, the absence of a light-induced increase in a signal II type spectrum, which could result from the interaction of tyr $Z^{\bullet}$ with an $S = 0$ state of the Mn cluster (see the Discussion for further considerations).

DISCUSSION

Assignment of the g = 2.035 Signal. The phenomenology of the production of the $g = 2.035$ signal bears strong similarities to the trapping of a metalloradical signal during excitation of the S_3 state by NIR light (*29*). In that case, the signal was assigned to $Y_Z^{\bullet}$ magnetically interacting with the Mn cluster in a singly deprotonated S_2 configuration. This present signal is also assigned to $Y_Z^{\bullet}$ magnetically interacting with the S_1 state. The arguments in support of this assignment are the following. The same transient species appears as an intermediate in the forward (charge separation), S_1 to S_2 (*32*), and the backward (charge recombination), S_2 to S_1, transition (this work), and tyr Z is the natural intermediate of the S state transitions. The broadened shape and the saturation

Scheme 1: Tentative Flowchart Summarizing the Observations of This and Earlier Papers[a]

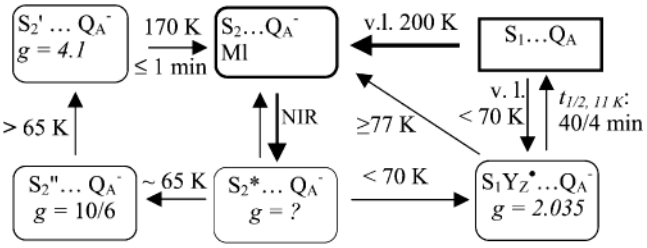

[a] Excitation by NIR light of the S_2 state results in the formation of a hypothetical excited state S_2*, which at elevated temperatures returns progressively to S_2 via high-spin intermediates (*34*). At liquid helium temperatures, S_2* converts predominantly to the metalloradical intermediate, $S_1Y_Z^{\bullet}$ (this work). This is the same intermediate that is produced by visible-light excitation of the S_1 state (*32*). See the text for details about the two half-time constants given for the $S_1Y_Z^{\bullet}\cdots Q_A^-$ to $S_1\cdots Q_A$ step, and about the thermal barriers affecting the decay of the $S_2^*\cdots Q_A^-$ state along the two different pathways. The S_2 state is assumed for simplicity to be characterized by the Mn multiline EPR signal, Ml, only. See Materials and Methods for a description of the NIR and visible-light (v.l.) illuminations.

properties of the present and also of all the related metalloradical signals associated with the donor side (see the introductory section) indicate proximity to a fast relaxing species. Furthermore, the signals vary in shape depending on the oxidation state of the Mn cluster. Clearly, the signals must result from a species in the proximity of the Mn cluster. Of the known electron donors implicated in direct or side pathways of electron donation, Chl_Z and Car^+ (*48*−*54*) are rather far from the Mn cluster (*55*, *56*) and were shown to have radical EPR spectra independent of the presence or absence of Mn (*48*, *55*). Clearly, tyr Z is the only suitable candidate.

A Flowchart. The results of this and of the earlier related observations (*32*−*35*) are incorporated into the flowchart of Scheme 1. The chart starts at the upper right corner with the S_1 state. Visible-light excitation of S_1 at 200 K results in advancement to the S_2 state (horizontal step). The intermediate $S_1Y_Z^{\bullet}$ is too short-lived at this temperature, but it can be trapped by visible-light excitation of S_1 at liquid helium temperatures (right vertical step) (*32*). This intermediate recombines slowly at liquid helium temperatures (several to tens of minutes at 11 K) with Q_A^-. Transfer, however, to ≥77 K immediately after the illumination results in advancement to S_2 (diagonal transition) (*32*). It has been shown in the work presented here that the reverse pathway, S_2 to S_1, can also be activated at liquid helium temperatures. NIR excitation of the S_2 state induces the same metalloradical intermediate, $S_1Y_Z^{\bullet}$, which decays along the same routes, as shown in the lower right part of the diagram, albeit with somewhat different kinetics reflecting perhaps differences in the stability of Q_A^-.

The left side of the chart includes the original observations of Boussac et al. (*33*−*35*), who demonstrated that NIR excitation at cryogenic temperatures converts reversibly the multiline-exhibiting $S = {}^1/_2$ state to higher-spin states. At ~65 K, an $S \geq {}^5/_2$ intermediate with $g = 10$ and 6 EPR signals can be trapped. This is converted at higher temperatures to the "$g = 4.1$" configuration, which in turn decays to the multiline configuration at approximately 170 K and higher temperatures. It might be argued that the metalloradical intermediate and the high-spin configurations of S_2 evolve in sequence. The experiments of Boussac et al. suggested, however, that the $g = 4.1$ signal, generated at 140 K, is the result of two photochemical events. The visible light induces charge separation and the S_1 to S_2 (multiline) transition, and the NIR part of the illumination excites the S_2 multiline configuration to the $g = 4.1$ signal (*33*). It appears therefore that the high-spin configurations evolve along a pathway different from the one that produces the metalloradical state. The fact that the high-spin configurations evolve at higher temperatures than the metalloradical state may indicate the presence of a thermal activation barrier in the former case. This interpretation is similar to the observations relating to the NIR excitation of the S_3 state (*29*). Accordingly, NIR excitation of S_2 is assumed for simplicity to produce a single transient S_2*. S_2* decays along two independent pathways as shown in the flowchart of Scheme 1.

Scheme 2: Two Pathways of Formation of the S_1Y_Z• Intermediate and Proton Equilibria[a]

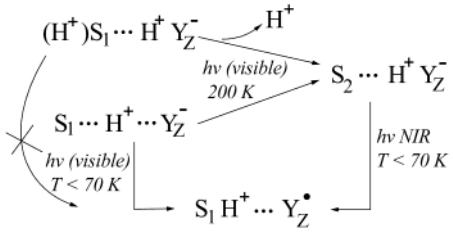

[a] S_1 is assumed to exist as a mixture of a protonated, $(H^+)S_1$, and a deprotonated, S_1, configuration.

The flowchart in Scheme 1 is simplified in a number of ways. The S_2 state is represented only by the configuration exhibiting the multiline signal. In many preparations, however, the $g = 4.1$ signal represents the stable configuration in a significant portion of centers. The situation with the $g = 4.1$ signal representing the ground state configuration in a number of centers and an NIR-excited configuration in centers exhibiting the multiline signal (see ref *57* for a thorough review of the $g = 4.1$ configuration) would be too complicated to consider here. The S_1 state is also heterogeneous, and this will be considered below in Scheme 2. Furthermore, not all steps in the flowchart can be optimally produced in a single type of preparation. Ethanol (2−3%, v/v) enhances the fraction of centers in the multiline configuration and allows for the clear observation of the spin transitions in spinach preparations (*33*, *34*). The presence of ethanol on the other hand precludes the observation of the metalloradical intermediate (ref *32* and this work). Furthermore, the $g = 4.1$ state cannot be trapped in cyanobacterial preparations, and the $g = 10/6$ state evolves at higher temperatures and with somewhat modified g values (*35*). The flowchart can be accordingly considered tentative at present and form the basis for future refinements. On the other hand, the chart presents an interesting analogy with the one characterizing the S_2 to S_3 transition (*29*) in stressing two important experimental facts. The tyr Z• intermediate can be trapped at liquid helium temperatures, and NIR excitation induces similar effects on S_2 and S_3: oxidation of the tyrosine by the Mn cluster and internal spin transitions in the Mn cluster. Insights into the unusual NIR sensitivity of both S_2 and S_3 are provided below.

NIR Sensitivity of the S_2 and S_3 States. Excitation of the Mn cluster in the S_2 and S_3 states with NIR light can result

in two different phenomena. It can cause spin state transitions (evolution of transient excited states characterized by new EPR signals at low magnetic fields) (see refs *34* and *35* for S_2 and refs *28* and *29* for S_3), or it can result in the oxidation of tyr Z, as described in detail here and in refs *28*, *29*, and *36*. Boussac et al. attributed the phenomenon of the spin state transitions in the S_2 state to either an intervalence charge transfer within a Mn(III)−Mn(IV) unit of the cluster (*33*) or a spin state transition of a Mn(III) atom from an $S = 2$ state (high-spin) to an $S = 1$ state (low-spin) (*34*). The phenomenon of the oxidation of tyr Z implies an NIR-induced increase in the oxidative capability of the Mn cluster.

An NIR electronic transition in O_2-evolving photosynthetic membranes was first noted by Dismukes and Mathis in the range of 730−900 nm, and this was found to correlate with the population of the S_2 state (*58*). The action spectrum of the NIR-induced spin state transitions in the S_2 state exhibits a broad maximum at ∼825 nm (*33*). The action spectrum of the NIR effects on S_3 or the induced oxidation of tyr Z was inferred to lie in the range of 700−900 nm (*28*). Recent experiments detected a weak NIR absorption band in the S_2 state that closely matches the action spectrum of the NIR-induced spin transitions in the S_2 state (*59*). These authors, on the basis of previous work (see below), assigned the NIR band to a d−d transition within the e_g orbitals of a Mn(III) atom of the cluster (*59*). NIR absorption bands have been observed in a number of six-coordinate monomeric Mn(III) complexes (*60*) and dimeric di-μ-oxo Mn(III)−Mn(IV) complexes (*61*). These bands have been attributed to spin-allowed d−d transitions within the levels of the E_g ground state of the d^4 Mn(III) ion, which are split due to Jahn−Teller distortion. In monomeric complexes, a D_{4h} symmetry was assumed and the band was assigned to the $^5B_{1g} \rightarrow {}^5A_{1g}$ transition (*60*). In the dimeric di-μ-oxo Mn(III)−Mn(IV) complexes, a symmetry of C_{2v} was assumed for the Mn_2O_2 core, and the NIR band was attributed to the $^5B_2 \rightarrow {}^5A_1$ transition (*61*).

Excitation of metal complexes by light absorption results in excited states, which possess considerably more stored energy; as a result, excited states may have different bond distances and angles, and larger vibrational and rotational energies. Markedly different redox potentials are observed between ground and excited states, too. Therefore, excited states exhibit a different driving force for electron transfer reactions; i.e., they are stronger oxidants and reductants than precursor ground states. This is exemplified by numerous studies on the photochemistry of Cr(III) and Ru(II) complexes (*62* and references therein). For example, the Cr(III)/Cr(II) redox potentials in a series of substituted polypyridine complexes, which lie in the region of −0.45 to −0.15 V, increased to 1.23−1.55 V upon illumination at ∼400 nm. That is, the Cr(III)*/Cr(II) couple, where Cr(III)* represents the excited state, became more oxidative by approximately 1.7 V (*63*). Furthermore, electronically excited Re(I), coupled to azurin (*64*), and Ru(II), in a supramolecular complex containing tyrosine (*65*), were shown to act as powerful reductants by donating one electron to an electron-accepting sink; their oxidized states afterward caused the formation of tyrosyl radicals in high yields.

According to the above discussion, the redox potential of the excited state of an Mn(III) atom can be estimated as follows. Absorption of light at 825 nm (12 121 cm^{-1}) results in the formation of an initial excited state, which promptly decays to a thermally relaxed excited state Mn(III)*. The energy of the latter can be roughly estimated to be ∼900 nm (11 111 cm^{-1}).

$$\mathrm{Mn(III)} \overset{h\nu}{\rightleftharpoons} \mathrm{Mn(III)^*} \quad (1)$$

$$\mathrm{Mn(III)} + e^- \rightleftarrows \mathrm{Mn(II)} \quad (2)$$

$$\mathrm{Mn(III)^*} + e^- \rightleftarrows \mathrm{Mn(II)} \quad (3)$$

Reaction 1 shows the excitation and relaxation to a thermally relaxed excited state Mn(III)*, which results in an energy gain of 1.4 eV (900 nm or 11 111 cm^{-1}). The free energy change (ΔG^*) of reaction 1 equals $-nE^*$. Thus, $E^* = -1.4$ V. The standard redox potential for reaction 2 [$E^0_{(III)/(II)}$] is not known. Reaction 3 can be obtained by subtracting reaction 1 from reaction 2. Therefore, the standard redox potential for reaction 3 [$E^0_{(III)*/(II)}$] is calculated with the relation $E^0_{(III)/(II)} - E^* = E^0_{(III)/(II)} + 1.4$ V. This increase of 1.4 V represents an upper limit, since some loss of absorbed energy due to reorganization of the excited state may occur. Hence, the Mn cluster upon NIR light irradiation acquires a highly oxidative center, an excited Mn(III) atom, which is capable of abstracting an electron from the nearby tyr Z.

The fact that both the S_2 and S_3 states show the same sensitivity to NIR illumination suggests that there is a common Mn(III) which does not change oxidation state during the $S_2 \rightarrow S_3$ step. If it is assumed that in the S_1 state the cluster contains two Mn(III) and two Mn(IV) atoms [an assignment favored by most authors, but see ref *7* for the assumption of a four-Mn(III) arrangement], the above considerations add weight to the view of ligand-centered oxidation (*66*, *67*) as opposed to Mn oxidation (*68*, *69*) during the S_2 to S_3 transition. Evidence suggesting the presence of a radical in the S_3 state (*70*) has been discussed previously (*29*). It should be noted, however, that the possibility of equilibrium between ligand-centered oxidation and Mn-centered oxidation configurations cannot be excluded on the basis of the considerations presented here. Static or dynamic equilibria between heterogeneous configurations appear to be a characteristic feature of the precursor S_2 state.

The NIR sensitive Mn(III) atom should be potentially present in the S_1 state, too. In fact, in a recent resonance Raman scattering study, it was concluded that in the S_1 state there is an NIR electronic transition with a λ_{ex} of ∼820 nm (*71*). Preliminary experiments failed to produce an $S_0Z^{\bullet}$ transient upon low-temperature NIR excitation of the S_1 state (in a fashion similar to formation of the $S_1Z^{\bullet}$ intermediate by NIR illumination of the S_2 state). Such an intermediate might be short-lived due to the redox potential of the S_1 state being lower than that of the S_2 state (*72*). Recently, however, what is most likely an $S_0Z^{\bullet}$ intermediate has been obtained by visible-light excitation of the S_0 state at liquid helium temperatures (J. H. A. Nugent, personal communication; C. Zhang and S. Styring, personal communication). It is possible then that the NIR excitation energy is dissipated within the Mn cluster [formation, e.g., of a Mn(II)−Mn(IV) short-lived transient] in the low-valence S_1. More experiments are, however, required in this direction.

Magnetic Interaction between S_1 and tyr Z•. The S_1 state can be prepared in a diamagnetic or a paramagnetic configuration (*43*, *44*). Two different types of integer spin EPR signals have been detected in the paramagnetic S_1 configuration by parallel-mode EPR: an ~600 G broad EPR signal centered at $g = 4.8$ (*44*, *45*) and a multiline signal centered at $g = 12$ (*46*). The latter has been detected initially in PSII preparations from the cyanobacterium *Synechocystis* sp. PCC6803 (*46*) and subsequently in spinach preparations depleted of the 23 and 17 kDa extrinsic polypeptides (*47*). In the present case, the same radical spectrum is obtained in a different cyanobacterial species and in a spinach preparation. The radical is broadened by a magnetic interaction, but it is not clear what is the spin of the Mn cluster that is causing the broadening of the spectrum. Yamauchi et al. concluded that the $g = 4.8$ signal originates from an $S = 1$ excited state separated by 2.5 K from the $S = 0$ ground state (*45*). Presumably, the $S = 1$ state could be the state that interacts magnetically and broadens the radical signal. The dominant fraction of centers should, however, be in the $S = 0$ state and exhibit an unperturbed radical signal from tyr Z•. Careful experiments in the $g = 2$ region showed no changes in the level of signal II during the production and subsequent decay of the S_1Y_Z• signal. It is unlikely that the expected weak coupling between the tyrosine and the Mn cluster (*22*) would affect considerably the magnetic structure of the Mn cluster. It is possible, however, that oxidation of tyr Z modifies the Mn cluster via electrostatic interactions, as the following considerations imply.

Insights into the Protonation State of S_1. The identical appearance of the radical signals, whether produced by NIR excitation of S_2 or by visible-light excitation of S_1, implies a similar configuration of S_1 in the two cases. It is reasonable to assume that the Mn(II) formed by the NIR-induced reduction of Mn(III) is rapidly reoxidized by a Mn(IV) ion to yield the normal S_1 configuration. It has been observed, furthermore, that in a given preparation no correlation exists between the efficiencies of the NIR-induced S_2 to S_1Y_Z• transition and the forward advancement of S_1 to the same metalloradical intermediate at 4.2 K. In *S. vulcanus*, for example, the NIR effect on S_2 is very pronounced, while the efficiency of the S_1 to S_1Y_Z• advancement at 4.2 K is very low (data not shown). These observations can be explained by the ideas outlined in ref *29* and the following considerations. An important limitation of the S state advancement at low temperatures is the inefficiency of the deprotonation step that accompanies most S state transitions. The S_1 to S_2 transition at ambient temperature is known to be accompanied in most preparations by a fraction of one proton loss on average (*73*, *74*). This implies that a fraction of centers does not lose a proton upon advancement to S_2. It is reasonable accordingly to assume that S_1 exists in a mixture of a protonated, $(H^+)S_1$, and a deprotonated, S_1, configuration. Furthermore, since Mn is proposed to serve as the proton acceptor upon tyr Z oxidation,[2] only the deprotonated fraction of S_1 will advance to S_1Y_Z• during visible-light illumination at liquid He temperatures. On the other hand, all fractions advance to S_2 by illumination at ≥200 K, since the protonated S_1 fraction can displace its proton at these elevated temperatures. The NIR-induced S_2 to S_1Y_Z• transition does not require the net loss of a proton, but a proton (and electron) transfer from tyr Z to the Mn cluster over a hydrogen bonding distance; it is accordingly not limited by the same restrictions that apply to the S_1 to S_1Y_Z• transition. These ideas are illustrated in Scheme 2.

Clearly, the same $S_1H^+\cdots Y_Z$• configuration is trapped via both pathways. The extent of protonation and the site of protonation of the Mn cluster in this intermediate state are different from both starting S_1 configurations (the simplified notation S_1Y_Z• used throughout this paper is misleading in this respect), and this may affect its magnetic properties as implied in the previous paragraph. The above considerations are entirely analogous to the trapping of the transient state $S_2'Y_Z$• by NIR excitation of the S_3 state or by white-light illumination of S_2' (*29*). S_2' is the decay product of S_3 at cryogenic temperatures, and represents a deprotonated S_2 state $S = {}^7/_2$ configuration (*30*). Unlike the deprotonated S_1 configuration which can represent a significant fraction of centers, S_2' must represent a negligible fraction of the S_2 state under normal conditions, since the S_2 to S_3 advancement in a variety of preparations is always accompanied by the net loss of one proton. Accordingly, visible-light excitation of S_2 at 4.2 K fails to produce detectable levels of the tyrosyl transient $S_2'Y_Z$•.

[2] It is suggested in ref *75* that the Mn cluster in S_1 contains a basic side and this acts as the acceptor of the tyr Z proton during the S_1 to S_2 transition in a fraction of centers (His 190 is the postulated proton acceptor on all other transitions). In ref *29*, it is proposed that the Mn cluster acts as the proton acceptor on all S state transitions.

ACKNOWLEDGMENT

We thank Dr. Asako Kawamori for her suggestion and help in using the cyanobacterial preparations. We also thank Dr. Harry Gray for discussions and in particular for pointing out that excited Mn(III) likely will be a powerful oxidant and could in principle oxidize a nearby tyrosine.

REFERENCES

1. Britt, R. D. (1996) in *Advances in Photosynthesis: Vol. 4 Oxygenic Photosynthesis: The Light Reactions* (Ort, R. D., and Yocum, C. F., Eds.) pp 137−164, Kluwer Academic Publishers, Dordrecht, The Netherlands.
2. Diner, B. A., and Babcock, G. T. (1996) in *Advances in Photosynthesis: Vol. 4 Oxygenic Photosynthesis: The Light Reactions* (Ort, R. D., and Yocum, C. F., Eds.) pp 213−247, Kluwer Academic Publishers, Dordrecht, The Netherlands.
3. Bricker, T. M., and Ghanotakis, D. F. (1996) in *Advances in Photosynthesis: Vol. 4 Oxygenic Photosynthesis: The Light Reactions* (Ort, R. D., and Yocum, C. F., Eds.) pp 113−136, Kluwer Academic Publishers, Dordrecht, The Netherlands.
4. Debus, R. J. (1992) *Biochim. Biophys. Acta 1102*, 269−352.
5. Yachandra, V. K., Sauer, K., and Klein, M. P. (1996) *Chem. Rev. 96*, 2927−2950.
6. Yocum, C. F., and Pecoraro, V. L. (1999) *Curr. Opin. Chem. Biol. 3*, 182−187.
7. Carrell, T. G., Tyryskin, A. M., and Dismukes, G. C. (2002) *J. Biol. Inorg. Chem. 7*, 2−22.
8. Boussac, A., Zimmermann, J. L., and Rutherford, A. W. (1989) *Biochemistry 28*, 8984−8989.
9. Sivaraja, M., Tso, J., and Dismukes, G. C. (1989) *Biochemistry 28*, 9459−9464.
10. Ono, T., and Inoue, Y. (1990) *Biochim. Biophys. Acta 1020*, 269−277.
11. Baumgarten, M., Philo, J. S., and Dismukes, G. C. (1990) *Biochemistry 29*, 10814−10822.
12. Andreasson, L. E., and Lindberg, K. (1992) *Biochim. Biophys. Acta 1100*, 177−183.
13. Hallahan, B. J., Nugent, J. H. A., Warden, J. T., and Evans, M. C. W. (1992) *Biochemistry 31*, 4562−4573.

14. MacLachlan, D. J., and Nugent, J. H. A. (1993) *Biochemistry 32*, 9772−9780.
15. Szalai, V. A., and Brudvig, G. W. (1996) *Biochemistry 35*, 1946−1953.
16. Astashkin, A. V., Mino, H., Kawamori, A., and Ono, T. (1997) *Chem. Phys. Lett. 272*, 506−516.
17. Gilchrist, M. L., Ball, J. A., Randall, D. W., and Britt, R. D. (1995) *Proc. Natl. Acad. Sci. U.S.A. 92*, 9545−9549.
18. Tang, X.-S., Randall, D. W., Force, D. A., Diner, B. A., and Britt, R. D. (1996) *J. Am. Chem. Soc. 118*, 7638−7639.
19. MacLachlan, D. J., Nugent, J. H. A., Warden, J. T., and Evans, M. C. W. (1994) *Biochim. Biophys. Acta 1188*, 325−334.
20. Peloquin, J. M., Campbell, K. A., and Britt, R. D. (1998) *J. Am. Chem. Soc. 120*, 6840−6841.
21. Dorlet, P., Di Valentin, M., Babcock, G. T., and McCracken, J. L. (1998) *J. Phys. Chem. B 102*, 8239−8247.
22. Lakshmi, K. V., Eaton, S. S., Eaton, G. R., Frank, H. A., and Brudvig, G. W. (1998) *J. Phys. Chem. B 102*, 8327−8335.
23. Dorlet, P., Boussac, A., Rutherford, A. W., and Un, S. (1999) *J. Phys. Chem B 103*, 10945−10954.
24. Hoganson, C. W., Lydakis-Simantiris, N., Tang, X.-S., Tommos, C., Warncke, K., Babcock, G. T., Diner, B. A., McCracken, J., and Striring, S. (1995) *Photosynth. Res. 46*, 177−184.
25. Hoganson, C. W., and Babcock, G. T. (1997) *Science 277*, 1953−1956.
26. Haumann, M., Mulkidjanian, A., and Junge, W. (1999) *Biochemistry 38*, 1258−1267.
27. Nugent, J. H. A., Turconi, S., and Evans, M. C. W. (1997) *Biochemistry 36*, 7086−7096.
28. Ioannidis, N., and Petrouleas, V. (2000) *Biochemistry 39*, 5246−5254.
29. Ioannidis, N., Nugent, J. H. A., and Petrouleas, V. (2002) *Biochemistry 41*, 9589−9600.
30. Ioannidis, N., and Petrouleas, V. (2002) *Biochemistry 41*, 9580−9588.
31. Geijer, P., Morvaridi, F., and Styring, S. (2001) *Biochemistry 40*, 10881−10891.
32. Nugent, J. H. A., Muhiuddin, I. P., and Evans, M. C. W. (2002) *Biochemistry 41*, 4117−4126.
33. Boussac, A., Girerd, J.-J., and Rutherford, A. W. (1996) *Biochemistry 35*, 6984−6989.
34. Boussac, A., Un, S., Horner, O., and Rutherford, A. W. (1998) *Biochemistry 37*, 4001−4007.
35. Boussac, A., Kuhl, H., Un, S., Rogner, M., and Rutherford, A. W. (1998) *Biochemistry 37*, 8995−9000.
36. Boussac, A., Sugiura, M., Inoue, Y., and Rutherford, A. W. (2000) *Biochemistry 39*, 13788−13799.
37. Berthold, D. A., Babcock, G. T., and Yocum, C. F. (1981) *FEBS Lett. 134*, 231−234.
38. Ford, R. C., and Evans, M. C. W. (1983) *FEBS Lett. 160*, 159−164.
39. Shen, J.-R., Ikeuchi, M., and Inoue, Y. (1992) *FEBS Lett. 301*, 145−149.
40. Shen, J.-R., and Inoue Y. (1993) *Biochemistry 32*, 1825−1832.
41. Petrouleas, V., and Diner, B. A. (1987) *Biochim. Biophys. Acta 893*, 126−137.
42. Szalai, V. A., Kühne, H., Lakshmi, K. V., and Brudvig, G. W. (1998) *Biochemistry 37*, 13594−13603.
43. Koulougliotis, D., Hirsh, D. J., and Brudvig, G. W. (1992) *J. Am. Chem. Soc. 114*, 8322−8323.
44. Dexheimer, S. L., and Klein, M. P. (1992) *J. Am. Chem. Soc. 114*, 2821−2826.
45. Yamauchi, T., Mino, H., Matsukawa, T., Kawamori, A., and Ono, T. (1997) *Biochemistry 36*, 7520−7526.
46. Campbell, K. A., Peloquin, J. M., Pham, D. P., Debus, R. J., and Britt, R. D. (1998) *J. Am. Chem. Soc. 120*, 447−448.
47. Campbell, K. A., Gregor, W., Pham, D. P., Peloquin, J. M., Debus, R. J., and Britt, R. D. (1998) *Biochemistry 37*, 5039−5045.
48. Hanley, J., Deligiannakis, Y., Pascal, A., Faller, P., and Rutherford, A. W. (1999) *Biochemistry 38*, 8189−8195.
49. Noguchi, T., Mitsuka, T., and Inoue, Y. (1994) *FEBS Lett. 356*, 179−182.
50. Pascal, A., Telfer, A., Barber, J., and Robert, B. (1999) *FEBS Lett. 453*, 11−14.
51. Deligiannakis, Y., Hanley, J., and Rutherford, A. W. (2000) *J. Am. Chem. Soc. 122*, 400.
52. Vrettos, J. S., Stewart, D. H., Cua, A., de Paula, J. C., and Brudvig, G. W. (1999) *J. Phys. Chem. B 103*, 6403−6406.
53. Faller, P., Thorsten, M., Rutherford, A. W., and MacMillan, F. (2001) *Biochemistry 40*, 320−326.
54. Tracewell, C. A., Cua, A., Stewart, D. H., Bocian, D. F., and Brudvig, G. W. (2001) *Biochemistry 40*, 193−203.
55. Faller, P., Pascal, A., and Rutherford, A. W. (2001) *Biochemistry 40*, 6431−6440.
56. Zouni, A., Witt, H.-T., Kern, J., Fromme, P., Krauss, N., Saenger, W., and Orth, P. (2001) *Nature 409*, 739−743.
57. Boussac, A., and Rutherford, A. W. (2000) *Biochim. Biophys. Acta 1457*, 145−156.
58. Dismukes, D. C., and Mathis, P. (1984) *FEBS Lett. 178*, 51−54.
59. Baxter, R., Krausz, E., Wydrzynski, T., and Pace, R. J. (1999) *J. Am. Chem. Soc. 121*, 9451−9452.
60. Davis, T. S., Fackler, J. P., and Weeks, M. J. (1968) *Inorg. Chem. 7*, 1994−2002.
61. Gamelin, D. R., Kirk, M. L., Stemmler, T. L., Pal, S., Armstrong, W. H., Penner-Hahn, J. E., and Solomon, E. I. (1994) *J. Am. Chem. Soc. 116*, 2392−2399.
62. Roundhill, D. M. (1992) *Photochemistry and Photophysics of Metal Complexes*, Plenum Press, New York.
63. Brunschwig, B., and Sutin, N. (1978) *J. Am. Chem. Soc. 100*, 7568−7577.
64. Di Billio, A. J., Crane, B. R., Wehbi, W. A., Kiser, C. N., Abu-Omar, M. M., Carlos, R. M., Richards, J. H., Winkler, J. R., and Gray, H. B. (2001) *J. Am. Chem. Soc. 123*, 3181−3182.
65. Sun, L., Burkitt, M., Tamm, M., Raymond, M. K., Abrahamsson, M., LeGourrierec, D., Frapart, Y., Magnuson, A., Kenez, P. H., Brandt, P., Tran, A., Hammarstrom, L., Styring, S., and Akerman, B. (1999) *J. Am. Chem. Soc. 121*, 6834−6842.
66. Roelofs, T. A., Liang, W., Latimer, M. J., Cinco, R. M., Rompel, A., Andrews, J. C., Sauer, K., Yachandra, V. K., and Klein, M. (1996) *Proc. Natl. Acad. Sci. U.S.A. 93*, 3335−3340.
67. Messinger, J., Robblee, J. H., Bergmann, U., Fernandez, C., Glatzel, P., Visser, H., Cinco, R. M., McFarlane, K. L., Bellacchio, E., Pizarro, S. A., Cramer, S. P., Sauer, K., Klein, M. P., and Yachandra, V. K. (2001) *J. Am. Chem. Soc. 123*, 7804−7820.
68. Ono, T. A., Noguchi, T., Inoue, Y., Kusunoki, M., Matsushita, T., and Oyanagi, H. (1992) *Science 258*, 1335−1337.
69. Iuzzolino, L., Dittmer, J., Dorner, W., Meyer-Klaucke, W., and Dau, H. (1998) *Biochemistry 37*, 17112−17119.
70. Ioannidis, N., Schansker, G., Barynin, V. V., and Petrouleas, V. (2000) *J. Biol. Inorg. Chem. 5*, 354−363.
71. Cua, A., Stewart, D. H., Reifler, M. J., Brudvig, G. W., and Bocian, D. F. (2000) *J. Am. Chem. Soc. 122*, 2069−2077.
72. Vass, I., and Styring, S. (1991) *Biochemistry 30*, 830−839.
73. Haumann, M., and Junge, W. (1996) in *Advances in Photosynthesis: Vol. 4 Oxygenic Photosynthesis: The Light Reactions* (Ort, R. D., and Yocum, C. F., Eds.) pp 165−192, Kluwer Academic Publishers, Dordrecht, The Netherlands.
74. Rappaport, F., and Lavergne, J. (2001) *Biochim. Biophys. Acta 1503*, 246−259.
75. Hoganson, C. W., and Babcock, G. T. (2000) in *Metals in Biological Systems* (Sigel, H., and Sigel, A., Eds.) Vol. 37, pp 613−656, Marcel Dekker, Inc., New York.

BI027051O